

Differential Effect of Anaerobic Digestion on Gaseous Products from Sequential Pyrolysis of Three Organic Solid Wastes

Lianpei Zou, Lin Song, Man Li, Xuan Wang, Xiang Huang, Yaning Zhang, Bin Dong, John Zhou, and Xiaowei Li*



Cite This: *ACS Omega* 2021, 6, 22103–22113



Read Online

ACCESS |



Metrics & More

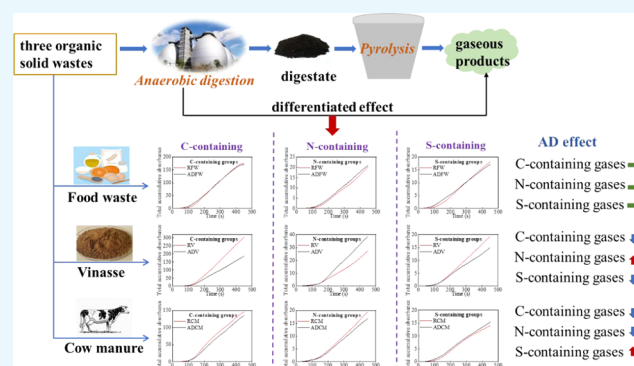


Article Recommendations



Supporting Information

ABSTRACT: Studies have shown that anaerobic digestion (AD) has an effect on the liquid and solid product property of sequential pyrolysis, but its influence on the gaseous products is lacking. In this study, syngas produced by pyrolysis from three raw organic solid wastes and the corresponding digestates, i.e., food waste, vinasse, and cow manure were investigated. AD causes a decrease in the contents of volatile solid, fixed carbon, C, H, and N and an increase in the S content. The weight loss of the wastes mainly occurs at 200–550 °C during the pyrolysis and the loss of the food waste and vinasse is higher than that of cow manure. In the carbon (C)-containing gas, AD leads to a decrease in the CH₄ content of the syngas, implying that the heat values of the digestates are lower than that of the raw substrates. After AD, the total amount of nitrogen (N)-containing gas from the vinasse increases by 40.1%, while that from cow manure decreases by 14.1%. On the contrary, the total amount of sulfur (S)-containing groups in the syngas from vinasse drop by 22.0%, while that from cow manure increases by 9.1%. In addition, slight changes in the C-, N-, and S-containing gases are found from food waste. The results indicate that AD has a different effect on the N- and S-containing gaseous groups from different organic solid wastes, and the mechanisms deserve further investigation. The findings supply a theoretical foundation for environmental-friendly application of syngas from the digestates.



1. INTRODUCTION

Food waste, vinasse, and cow manure are common organic solid wastes that come from municipal solid waste, industrial waste, and animal manure, respectively, and huge outputs have made them a serious environmental problem.^{1–3} If they are not treated in time and effectively, they pose a challenge to the ecological environment. Anaerobic digestion (AD) can not only realize the reduction of organic solid wastes but also effectively produce biomass fuels such as methane.⁴ However, 15–40% of the organic matter is used to produce biogas and most of the nutrients are stored in the digestates.^{5,6} The digestates may also be odorous, and contain toxic volatile fatty acids and emit greenhouse gases in the direct land application.⁷ Therefore, it may be necessary to post-treat digestates to ensure efficiency and safety.⁸

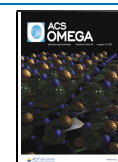
Pyrolysis is an effective technology to treat digestate, which can remove odor, pathogenic bacteria, and reduce greenhouse gas emissions.⁷ Moreover, pyrolysis can also reduce the weight and volume of the digestates and make full use of the biomass energy in the digestate.⁹ During the process, the organics of the digestate are disintegrated into useful products such as biochar, bio-oil, and syngas, which can be used as fuel, raw materials of various chemicals, and soil additives and adsorbents, respectively.^{9–11} Researchers reported that the performance

of pyrolysis products from the digestate is better than that of raw materials. Inyang et al.¹² found that the maximum lead adsorption capacity of biochars made from anaerobically digested sugarcane bagasse is far higher than that made from raw sugarcane bagasse. Liang et al.¹³ found that the content of phenolic compounds increases during the pyrolysis process of anaerobically digested rice straw, indicating that anaerobic digestion can increase the energy density of the bio-oil. However, the syngas from the pyrolysis of the digestate has been rarely reported. As an additional energy source, syngas can be burnt alone or mixed with anaerobic biogas to generate electricity/heat.¹⁴ However, there are some pollutants such as H₂S, HCl, and NH₃ in the syngas,¹⁵ causing the syngas needs to be refined before their application. Therefore, the gaseous composition of the syngas from the digestate pyrolysis deserves to be investigated to utilize it effectively and environmentally friendly.

Received: May 22, 2021

Accepted: August 6, 2021

Published: August 19, 2021



Meanwhile, some papers have reported the differences in pyrolysis products from different organics. Cantrell et al.¹⁶ found that the biochars are different in the specific surface area, ash, and nutrient contents from the pyrolysis of swine-separated solids, paved-feedlot manure, dairy manure, poultry litter, and turkey litter. Ateş et al.¹⁷ found that the yield of total aliphatic hydrocarbons in the pyrolysis oil of municipal plastic waste is higher than that of municipal solid waste at all temperatures. Fernández and Menéndez¹⁸ studied the syngas produced by the pyrolysis of glycerol, sewage sludge, and coffee hull and found that the value of H₂/CO in the syngas from sewage sludge is higher than from coffee hull, followed by glycerol. Zong et al.¹⁹ pyrolyzed starch, cellulose, hemicellulose, lignin, protein, and oil and found that their pyrolysis behavior and gaseous product evolution are different. Therefore, it is reasonable to speculate that the syngas produced by the pyrolysis from the digestates of different organic solid wastes is diverse. In addition, Li et al.²⁰ have shown that AD has a different effect on the pyrolysis kinetics of different organic substances, possibly due to different proportions of protein and carbohydrate groups in the substrates. Therefore, it is hypothesized that AD may pose a disparate effect on the syngas from sequential pyrolysis of the organic solid wastes such as food waste, vinasse, and cow manure due to their different biodegradation performances during anaerobic digestion.

C, N, and S are important elements of raw and anaerobically digested materials, and they produce most of the components in the syngas. The main components are CO, H₂, CO₂, CH₄, and H₂O as well as some organics such as light hydrocarbons, tar, and inorganic impurities such as H₂S, HCl, and NH₃.¹⁵ In C-containing groups, CO and CH₄ are combustible gases, which can be used to generate electricity and heat.²¹ In N-containing groups, NO_x can be easily produced from HNCO, HCN, and NH₃ through combustion, and these are important precursors of NO_x forming photochemical smog.²² In S-containing groups, H₂S and SO₂ can be converted into SO_x, which form photochemical smog and acid rain pollution during the combustion process of syngas.²³ Therefore, in this study, the C-, N-, and S-containing gaseous groups in the syngas from the pyrolysis of raw and anaerobically digested organic wastes were investigated to understand their resource and pollutant properties in depth.

Thermogravimetric analysis (TGA) is often used to investigate the changes of sample quality with temperature and time.²⁴ Fourier transform infrared spectroscopy (FTIR) detects functional groups and chemical structure of the biomass and its thermochemical conversion product structure, heteroatom function (mainly oxygen-containing), and mineral composition changes.²⁵ In this study, a combination of TGA and FTIR was applied to explore the effect of AD on the gaseous C-, N-, and S-containing gaseous products from the sequential pyrolysis of organic solid wastes.

The objectives of this study are (1) to reveal the effect of AD on chemical and pyrolysis characteristics of three organic solid wastes, i.e., food waste, vinasse, and cow manure and (2) to investigate the effect of AD on C-, N-, and S-containing gaseous products from their pyrolysis. This study will help to further understand the effect of AD on the sequential pyrolysis of different organics in depth and supply a theoretical basement for digestate-based syngas utilization.

2. MATERIALS AND METHODS

2.1. Substrates and Inoculums. Raw food waste (RFW) was taken from Xiyuan Canteen at Siping Campus of Tongji University in Shanghai city; raw vinasse (RV) was taken from the Guizhou Moutai Distillery in Guizhou province; and raw cow manure (RCM) was obtained from a dairy farm in the suburb of Pudong, Shanghai city. Inoculated sludge was taken from our previous anaerobic reactor.²⁶ Total solids of the RFW, RV, and RCM were 18–24, 43–47, and 18–22%, respectively.

2.2. AD Process and Material Analysis. The working volume of the anaerobic digestion reactor was 6 L, and it ran semicontinuously with an operating temperature of 35 ± 1 °C. The stirring speed was set to 60 rpm (rotations per minute), and the interval was 2 min after every 10 min of stirring. Feeding and discharging were performed once a day. The solid retention time (SRT) of the reactors for food waste, vinasse, and cow manure was all 30 days, and the solid content was set to 7, 10, and 20%, respectively.

After three SRTs, the reactors trended to become stable. In the stable periods, three kinds of digestates, i.e., anaerobically digested food waste (ADFW), anaerobically digested vinasse (ADV), and anaerobically digested cow manure (ADCM), were collected from the corresponding reactor outlet. Then, the raw and digestate samples were freeze-dried and sieved to 0.15 mm and then stored in a desiccator with a discolored silica gel for further analysis.

Moisture, ash, and volatiles of the samples were analyzed according to ASTM standards D1102, E871, and E872, respectively. The fixed carbon was measured as a difference. The elemental compositions of raw and anaerobically digested materials were measured using a Vario Micro element analyzer (Germany) with <0.1% abs analysis accuracy. X-ray photoelectron spectroscopy (XPS) analysis was conducted using an ESCALAB250Xi (Thermo Scientific, U.K.) spectrometer with non-monochromatic Al and K anode targets and a scan size of 0.1 eV per step.

2.3. Pyrolysis and TGA-FTIR. Thermogravimetric (TG) and FTIR data of the freeze-dried and sieved samples were carried out using a TGA8000 TG analyzer combined with a Frontier FTIR spectrometer fitted with a gas cell. Gas materials from TG analyzer were directly gathered in the gas cell and determined immediately through the FTIR spectrometer. The FTIR spectra (4000–500 cm⁻¹; resolution, 2 cm⁻¹) of the gases were obtained successively with the modified baseline. The whole gas flow path was wrapped with a heating wire to prevent the condensation of any volatile disintegration products.

The samples were pyrolyzed in helium conditions. The heating process was as follows: the samples were heated from 30 to 100 °C at a heating rate of 30 °C/min, then maintained at 100 °C for 10 min, and then heated to 850 °C at 100 °C/min. The carrier gas uses ultra-high purity helium with a purity of 99.99% and a constant flow rate of 100 mL/min. The weight of all samples was kept at 20 ± 2 mg.

The TG/derivate TG (DTG) data were analyzed using Pyris software (PerkinElmer, Inc., U.K.), and the FTIR spectral data were provided by TimeBase Version 3.1.0 software (PerkinElmer, Inc., U.K.).

2.4. Data Analysis. C-containing, N-containing, and S-containing components of syngas from all organic matters were identified based on the FTIR absorption peaks,^{26,27} which is

Table 1. Chemical Characteristics of the Raw and Anaerobically Digested Substrates

samples ^a	proximate analysis (wt %)				elemental analysis (wt %)						organic matter removal rate (%)
	moisture	volatile solid	fixed carbon	ash content	C	H	N	S	H/C	C/N	
RFW	6.5	79.5	6.8	7.1	48.6 ± 0.25	7.1 ± 0.04	3.5 ± 0.08	0.43 ± 0.10	1.8	16.4	83.2
ADFW	7.0	59.8	1.8	31.3	34.5 ± 0.36	5.7 ± 0.06	2.9 ± 0.11	0.79 ± 0.08	2.0	13.7	
RV	6.5	74.1	13.7	5.7	43.8 ± 0.25	6.0 ± 0.06	4.7 ± 0.09	0.26 ± 0.06	1.6	10.9	78.3
ADV	8.2	59.7	7.3	21.8	37.2 ± 0.15	5.3 ± 0.06	5.9 ± 0.10	0.72 ± 0.15	1.7	7.4	
RCM	7.1	56.4	8.5	28	33.0 ± 0.23	4.9 ± 0.05	3.0 ± 0.07	0.37 ± 0.07	1.8	12.8	51.1
ADCM	5.9	47.9	1.9	44.3	27.0 ± 0.21	4.2 ± 0.06	2.3 ± 0.06	1.2 ± 0.05	1.9	13.4	

^aRFW, raw food waste; ADFW, anaerobically digested food waste; RV, raw vinasse; ADV, anaerobically digested vinasse; RCM, raw cow manure; ADCM, anaerobically digested cow manure.

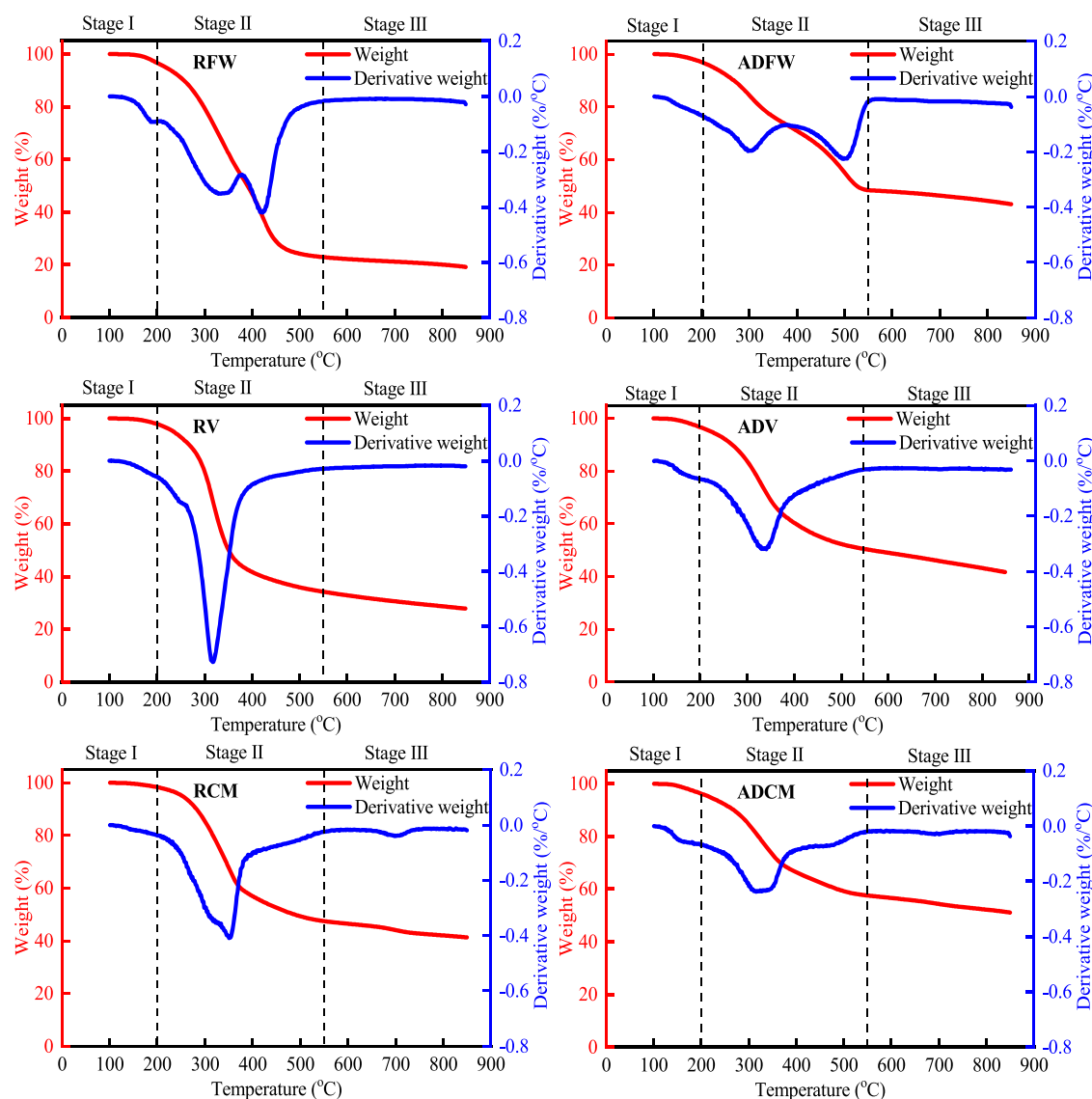


Figure 1. TG/DTG curves of the raw and anaerobically digested substrates. RFW, raw food waste; ADFW, anaerobically digested food waste; RV, raw vinasse; ADV, anaerobically digested vinasse; RCM, raw cow manure; ADCM, anaerobically digested cow manure.

outlined in Table S1. The area under the absorbance curve is directly proportional to the concentration of gas released during the pyrolysis.²⁸ The gas emission concentration in the pyrolysis process can be measured by integrating the absorbance (A) with the time (t), or it can be expressed by the accumulative absorbance. The accumulative absorbance $I_{A,t}$ at a specific t can be calculated as²⁸

$$I_{A,t} = \int_0^t A \, dt \quad (1)$$

where

$$\int_{t_1}^{t_2} A \, dt \approx \frac{(t_2 - t_1)(A_{t_1} + A_{t_2})}{2} \quad (2)$$

Table 2. Changes in DTG of the Raw and Anaerobically Digested Substrates^c

samples	stage I			stage II			stage III				
	T_1^a (°C)	DTG ₁ ^b (%/°C)	WL ₁ ^c (%)	T_2 (°C)	DTG ₂ (%/°C)	T_3 (°C)	DTG ₃ (%/°C)	WL ₂ (%)	T_4 (°C)	DTG ₄ (%/°C)	WL ₃ (%)
RFW	182	0.083	3.34	332	0.352	422	0.420	73.70	ND	ND	3.75
ADFW	ND ^d	ND	3.04	297	0.197	500	0.225	48.56	ND	ND	5.35
RV	ND	ND	2.13	317	0.728	ND	ND	63.66	ND	ND	6.41
ADV	ND	ND	3.36	327	0.319	ND	ND	46.20	704	0.031	8.73
RCM	ND	ND	1.67	350	0.408	ND	ND	50.82	702	0.039	6.18
ADCM	175	0.061	3.76	315	0.237	ND	ND	38.64	700	0.029	6.46

^a T_1 , T_2 , T_3 , T_4 , the temperatures according to the first, second, third, and fourth peak, respectively. ^bDTG₁, DTG₂, DTG₃, DTG₄, the mass loss rates according to the first, second, third, and fourth peak, respectively. ^cWL₁, WL₂, WL₃, the weight losses at stage I, stage II, and stage III, respectively. ^dND, no data. ^eRFW, raw food waste; ADFW, anaerobically digested food waste; RV, raw vinasse; ADV, anaerobically digested vinasse; RCM, raw cow manure; ADCM, anaerobically digested cow manure.

The integral absorbance value consequently does not represent an absolute value of absorbance but the absorbance multiplied for the time in seconds. The value remains proportional to the total gas released.²⁷ The emission content of C-containing gaseous products was the sum of the accumulative absorbance of CH₄, CO, CO₂, CH₃OH, CH₃CHO, and CH₃COOH. The emission content of N-containing gaseous products was the sum of the accumulative absorbance of HNCO, HCN, NH₃, and NO. The emission content of S-containing gaseous products was the sum of the accumulative absorbance of H₂S, SO₂, and COS.

3. RESULTS AND DISCUSSION

3.1. Effect of AD on Chemical Characteristics of These Substrates. Chemical characteristics of raw and anaerobically digested substrates are shown in Table 1. Volatile solids of RFW, RV, and RCM are 79.5, 74.1, and 56.4%, respectively, and decrease by 83.2, 78.3, and 51.1% after AD, respectively. The difference in the removal rates of organic matter mainly relates to their chemical composition. Food waste and vinasse mainly consist of various easily degradable organic substances such as carbohydrates, lipids, and protein while cow manure is relatively resistant to AD due to the high lignocellulosic contents (cellulose, hemicellulose, and lignin).^{29–31} Fixed carbon is a solid combustible residue after heating and an important indicator for evaluating the quality of solid fuels.³² The contents of fixed carbon in all substrates decrease after AD, while that of the ash increases. Lower fixed carbon means higher volatile solids and C-containing compounds.³³ Compared with raw materials, C and H content and C/N ratio of anaerobically digested materials decrease except for C/N of cow manure, but the H/C ratio increases to different degrees. The increase in the H/C ratios indicates that the degree of aromatization and carbonization has decreased, this may be because the short digestion time leads to a moderate decrease in aromaticity.³⁴ In addition, the proportion of sulfur in the anaerobically digested materials is all increased while nitrogen in the anaerobically digested materials is all decreased except ADV. This result indicates that AD promotes the reduction of C- and N-containing contents and the enrichment of S-containing groups.

3.2. Effect of AD on Pyrolysis Characteristics of These Substrates. TG/DTG curves of the three organic solid wastes and their digestates are shown in Figure 1, while their specific pyrolysis parameters are shown in Table 2. TG curves of three organic solid wastes and corresponding digestates are similar, while some differences exist among the DTG curves.

The DTG curves are all divided into three different stages. In the first stage, the weight loss begins at 100 °C, and the peak weight loss occurs around 180–200 °C, and the weight loss ranges from 1.67 to 3.76%. There is a slight difference in weight loss at this stage among the three organics. The weight loss at this stage is the result of the evaporation of physically adsorbed water and light volatiles.³⁵ The weight loss in the first stage is not obvious, since the organic matter has been fully dried before the experiment.³⁴

In the second stage, as shown in Tables 1 and 2, the rates of weight loss of the substrates during the temperature of 200–550 °C range from 38.64 to 73.70%, approximating to their contents of volatile solid. This result indicates that the second stage is the main weight-loss stage and mainly attributed to the degradation of volatile matter.³⁴ AD has no obvious effect on the trend of TG/DTG curves but causes a decrease in the weight loss of digestates, corresponding to the previous research results.³⁶ The reason is that the organic matter decreases and the residual groups become difficult to crack after AD (Table 1). The weight-loss rates of RFW (73.70%) and RV (63.66%) are greater than that of RCM (50.82%). Accordingly, those of ADFW (48.56%) and ADV (46.20%) are also greater than that of ADCM (38.64%), consistent with the volatile solids shown in Table 1. Except for RFW and ADFW, other substrates have only one peak in the DTG curves in the second stage. The first peak of weight loss of RFW and ADFW occurs with temperature at 300–350 °C, associated with the degradation of protein, starch, lipid, sugar, hemicellulose, and cellulose.^{20,34} The second weight-loss peaks of RFW and ADFW occur at 422 and 500 °C, respectively, possibly related to the decomposition of lignin.³⁷ Notably, compared with food waste and cow manure, the weight of vinasse declines rapidly at a rate of 0.728%/°C at temperature of 300–400 °C in the second stage (Figure 1). The possible reason is that the organic matter of vinasse are mainly made of sugars, carbohydrates, lipids, and protein, which are easy to degrade.³⁰

In the third stage, there is a slight mass change in pyrolysis behavior, and the weight drops by 3.75–8.73% at 550–900 °C. A slight difference is found in weight loss for all substrates in the third stage, and all substrates are below 10%. This may be the result of the decomposition of the carbonaceous material remaining in the residue.³⁴ In this stage, the weight loss of raw materials is higher than that of the digestate after AD, consistent with the previous results.²⁰ The ash content of all of the three substrates increase after AD (Table 1). A research reported that the main components of ash may consist of inorganic substances such as calcium, sodium, potassium, magnesium, and silicon.³⁸ This also indicates that unstable

Table 3. Changes in Accumulative Absorbance of the Raw and Anaerobically Digested Substrates^a

groups	components	RFW	ADFW	variation (%)	RV	ADV	variation (%)	RCM	ADCM	variation (%)
C-containing gases	CH ₄	14.71	11.95	-18.8	11.03	7.38	-33.1	8.51	6.17	-27.5
	CO	0.26	0.27	2.8	0.07	0.10	44.8	0.14	0.16	17.6
	CO ₂	124.17	102.21	-17.7	262.34	145.30	-44.6	104.13	85.22	-18.2
	CH ₃ OH	4.44	5.91	33.3	3.29	5.94	80.5	4.13	4.03	-2.5
	CH ₃ CHO	17.75	24.61	38.7	15.14	13.87	-8.4	14.50	18.09	24.8
	CH ₃ COOH	15.23	27.32	79.4	13.13	12.91	-1.7	15.07	21.43	42.2
	total	176.55	172.28	-2.4	304.99	185.50	-39.2	146.48	135.10	-7.8
N-containing gases	HNCO	4.06	3.21	-20.9	8.44	5.03	-40.4	2.83	2.40	-15.3
	HCN	8.91	9.09	2.1	12.08	12.28	1.6	9.28	7.30	-21.3
	NO	0.95	0.67	-29.5	1.49	0.71	-52.2	0.55	0.56	0.8
	NH ₃	6.49	8.07	24.5	5.43	20.42	276.2	6.86	6.52	-4.9
	total	20.40	21.05	3.1	27.44	38.45	40.1	19.52	16.78	-14.1
S-containing gases	SO ₂	11.51	11.00	-4.4	12.98	9.28	-28.5	8.77	9.59	9.3
	H ₂ S	4.32	3.90	-9.7	3.37	2.33	-30.8	3.29	3.66	11.5
	COS	2.37	2.28	-3.7	2.85	3.38	18.5	1.97	2.05	4.1
	total	18.19	17.18	-5.6	19.21	14.99	-22.0	14.03	15.30	9.1

^aRFW, raw food waste; ADFW, anaerobically digested food waste; RV, raw vinasse; ADV, anaerobically digested vinasse; RCM, raw cow manure; ADCM, anaerobically digested cow manure.

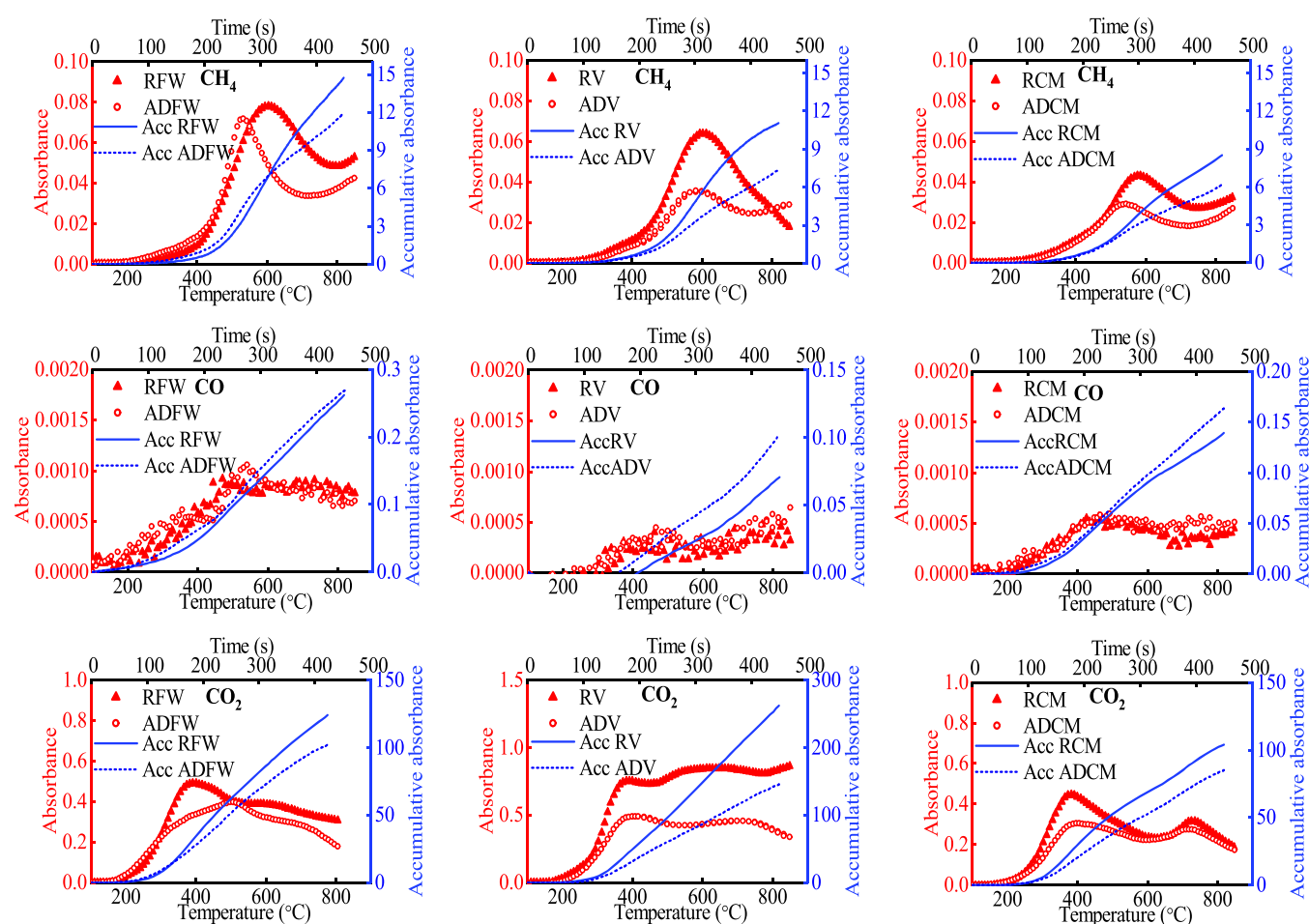


Figure 2. Changes in C-containing gaseous products during pyrolysis. RFW, raw food waste; ADFW, anaerobically digested food waste; RV, raw vinasse; ADV, anaerobically digested vinasse; RCM, raw cow manure; ADCM, anaerobically digested cow manure. Acc, accumulative.

organic matter is degraded, while inorganic matter and some refractory organic matter are relatively enriched during AD.²⁰

3.3. Effect of AD on Gaseous Products of These Substrates. The syngas produced by the pyrolysis of organic matter can be utilized as fuel, but there are some pollutants in

the syngas. For example, C-containing groups such as CH₄ in syngas can be utilized as heat and electricity through combustion. The presence of N-containing groups NO_x may form photochemical smog. S-containing groups may be converted into sulfur compounds, causing photochemical

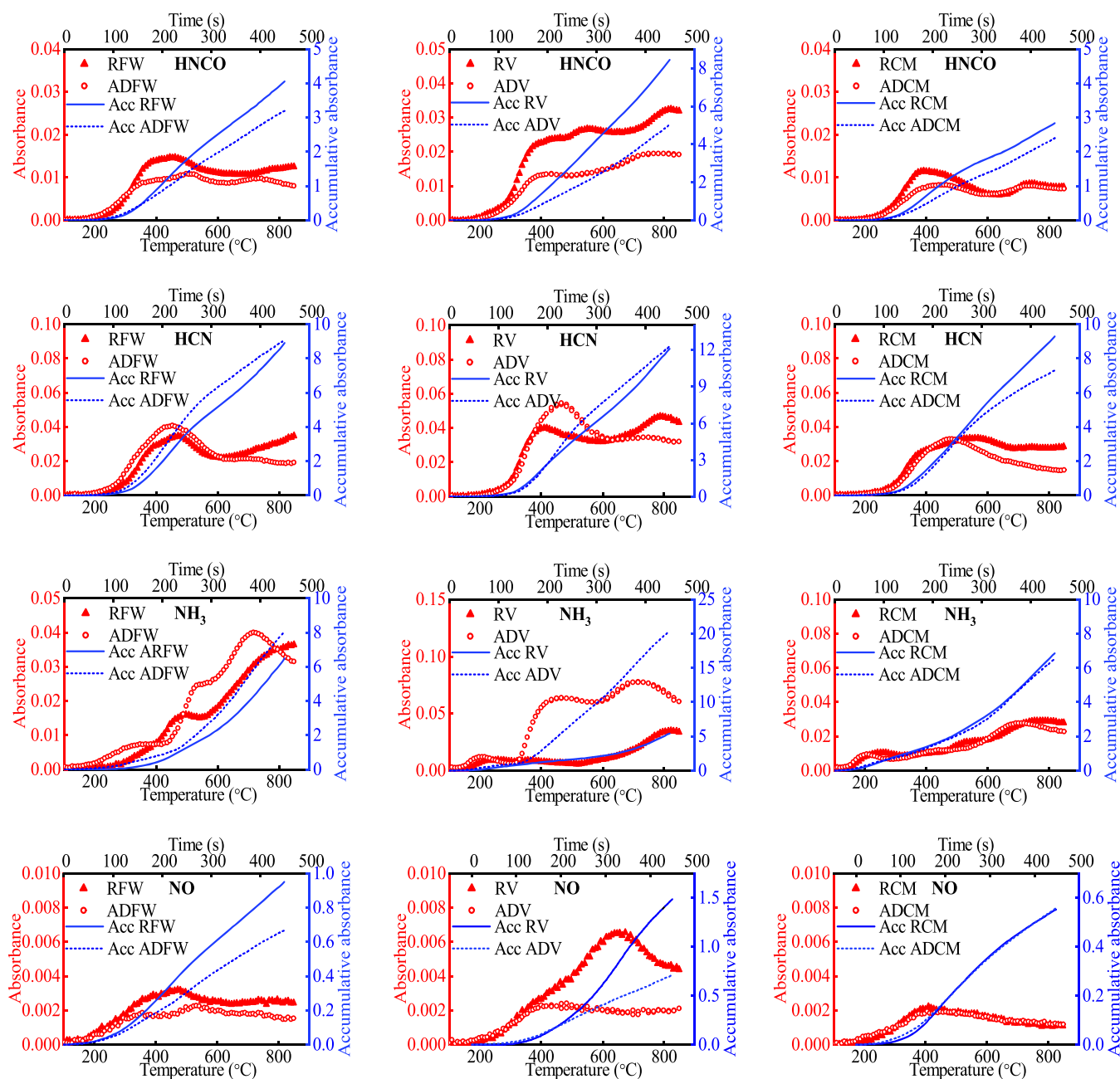


Figure 3. Changes in N-containing gaseous products during pyrolysis. RFW, raw food waste; ADFW, anaerobically digested food waste; RV, raw vinasse; ADV, anaerobically digested vinasse; RCM, raw cow manure; ADCM, anaerobically digested cow manure. Acc, accumulative.

smog and acid rain pollution. Therefore, effect of AD on C-, N-, and S-containing pyrolysis gaseous products were respectively investigated in the three organic wastes, and the results are outlined in Table 3.

3.3.1. Gaseous C-Containing Groups. Instantaneous and accumulative absorbance changes in C-containing gaseous products of all substrates at different temperatures are shown in Figure 2. C-containing products originate from the decomposition of various C-containing organic matter such as carbohydrates, lipids, proteins, polysaccharides, etc. Compared with raw substrates, the accumulative absorbance of C-containing gaseous products from ADFW, ADV, and ADCM decrease by 2.4, 39.2, and 7.8%, respectively, corresponding to the results that the carbon contents in RFW, RV, and RCM all decrease after AD shown in Table 1.

Compared with other substrates, the C-containing gases from ADV have a more significant decrease, possibly due to more easily degradable C-containing compounds in the RV.³⁰

CH₄ is the main combustible component of syngas. As shown in Figure 2, the peak temperature of CH₄ from all digestates is lower than that from the raw materials. Compared with raw materials, the CH₄ accumulative absorbance of all of the ADFW, ADV, and ADCM have a large decline with the values of 18.8, 33.1, and 27.5%, respectively. The formation of CH₄ is mainly related to the random cleavage of aliphatic side chains, the decomposition of -OCH₃ and C=C groups, and the secondary cleavage of volatiles at high temperatures.¹⁹ This may be related to the fact that some macromolecular organics are transformed into low-molecular-weight groups.²⁰

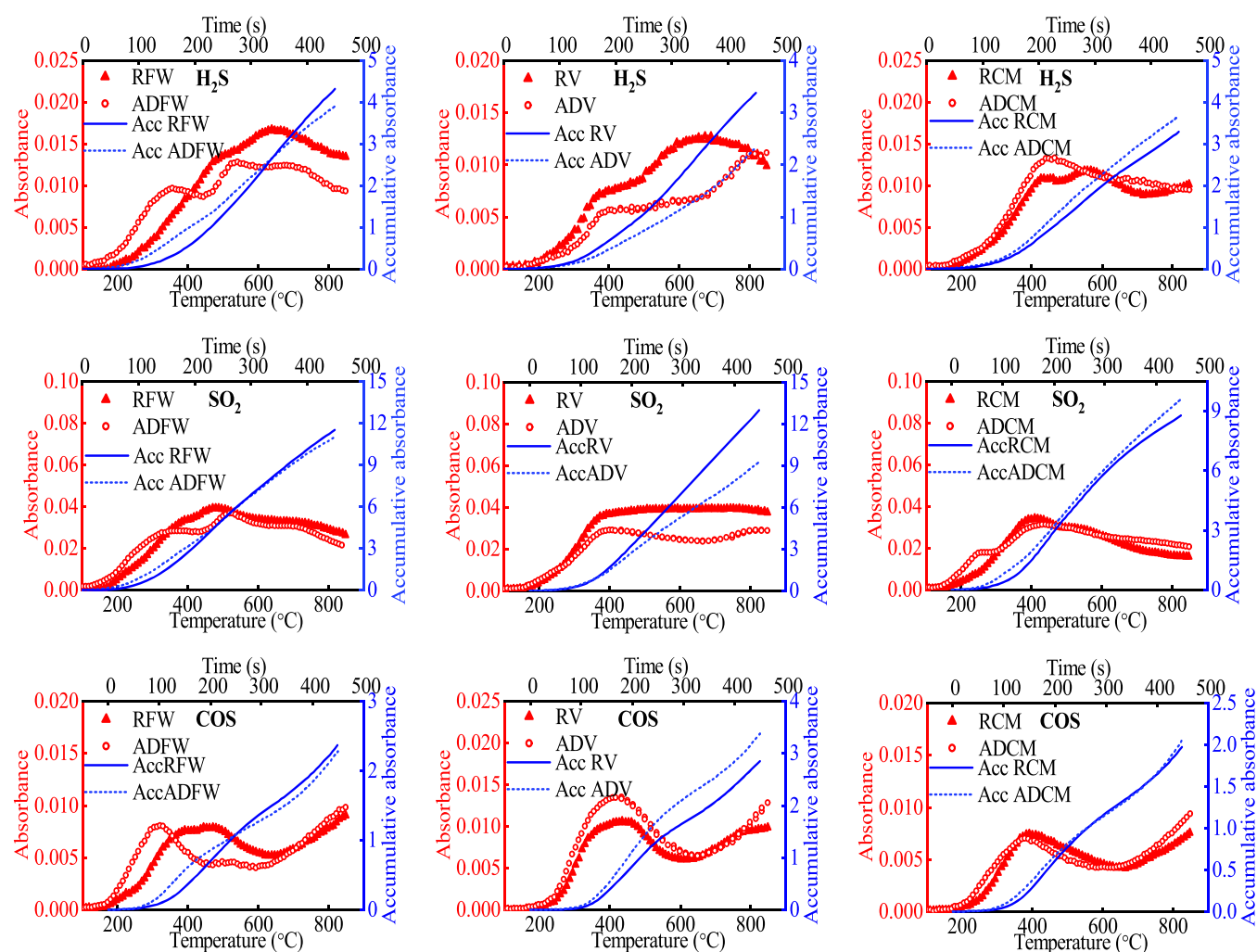


Figure 4. Changes in S-containing gaseous products during pyrolysis. RFW, raw food waste; ADFW, anaerobically digested food waste; RV, raw vinasse; ADV, anaerobically digested vinasse; RCM, raw cow manure; ADCM, anaerobically digested cow manure. Acc, accumulative.

CO_2 instantaneous absorbance shows a clear bimodal trend in RCM and ADCM (Figure 2). The first peak, which is the main production stage of CO_2 , occurs at temperatures between 300 and 500 °C, related to the fracture of the unstable chemical bond $\text{C}=\text{O}$ and COOH .³⁹ The second peak comes mainly from the degradation of carbonate corresponding to the third stage of pyrolysis (Figure 1).³⁹ This is consistent with the previous results.⁴⁰ As shown in Figure 2 and Table 3, CO_2 from RFW, RV, and RCM decrease by 17.7, 44.6, and 18.2% after AD, respectively. During the AD, 15–40% of the organic matter is used to produce biogas, and CH_4 and CO_2 is the main component of biogas.⁵ The reason why CH_4 and CO_2 from the pyrolysis of digestates decrease is that some organic matter is degraded in the AD and organic matter remaining in the digestates is reduced.⁶ Compared with ADFW and ADCM, ADV has a higher reduction. The possible reason is that ADV contains more easily degradable C-containing organic compounds.

Compared with raw materials, CO from ADFW, ADV, and ADCM all increase with the value of 2.8, 44.8, and 17.6%, respectively. CO comes from the fracture of the unstable chemical bond $\text{C}=\text{O}$ and COOH and the chemical reaction of CO_2 and coke.³⁹ The CO content in the syngas is low, accounting for less than 0.2%, so the influence of CO on the calorific value of the syngas is negligible.

The instantaneous and accumulative absorbance of CH_3OH , CH_3CHO , and CH_3COOH are shown in Figure S1. AD causes an increase in the accumulative absorbance of CH_3OH in RFW and RV by 33.3 and 80.5%, respectively, and a decrease in the RCM by 2.5% and an increase in the accumulative absorbance of CH_3CHO in RFW and RCM by 38.7 and 24.8%, respectively, and a decrease in RV by 8.4% (Figure S1). Compared with the raw substrates, the accumulative absorbance of CH_3COOH in ADFW and ADCM also increases by 79.4 and 42.2%, respectively, and a slight change is found in ADV. The possible reason is that some low-molecular-weight substances such as volatile organic solids remain in the digestates after AD.⁴¹

3.3.2. Gaseous N-Containing Groups. The instantaneous and accumulative absorbance changes in N-containing gaseous products from all substrates at different temperatures are depicted in Figure 3 and Table 3. Compared with raw materials, the accumulative absorbance of N-containing gaseous products increases by 40.1% from ADV and decreases by 14.1% from ADCM and do not obviously change from ADFW. The results show that the concentration of N-containing gas from vinasse increases but that from cow manure decreases after AD. Proteins in the organic wastes are the main source of N-containing gas generated by pyrolysis.⁴² The accumulative absorbance of N-containing gas is consistent

with the variation of nitrogen content in the substrates. As shown in Table 1, the nitrogen in vinasse increases from 4.69 to 5.90 wt %, and the nitrogen in cow manure decreases from 3.00 to 2.35 wt % after AD. The possible reason is that cow manure contains so much crude fiber content (43.33%) while protein content is low³¹ and thus less N-containing gas is produced.

HCN and NH₃ are the most important N-containing gas, which can account for 63.8–85.1% in the pyrolysis of the three organic compounds and their digestates. HCN from food waste, vinasse, and cow manure undergoes different changes after AD. The HCN concentrations of ADFW and ADV are higher than that of the corresponding raw substrates at 300–600 °C and lower after 600 °C, while the HCN concentration of ADCM is close to that of RCM before 550 °C and lower than that of RCM after 550 °C. On the whole, accumulative absorbances of HCN from RFW and RV have a 2.1 and 1.6% increase, respectively, while that from RCM has a 21.3% decrease after AD. HCN originates from the cracking of volatile cyclic amides released by proteins at low temperatures and from the thermal decomposition of cyano aromatics in tar at high temperatures.²² This is consistent with previous results.¹⁹ Compared with food waste and vinasse, cow manure is low in protein and rich in cellulose, hemicellulose, and lignin,³¹ implying that HCN only came from the cleavage of cyano aromatic compounds in tar after 550 °C. The possible reason for the decrease in HCN from cow manure is the degradation of protein during the AD process.⁴⁴

The NH₃ yield of ADV pyrolysis under 300 °C accounts for 4.25% of the total yield, mainly derived from the decomposition of ammonium nitrogen or protein nitrogen.⁴³ The yield of NH₃ from ADV suddenly rises very rapidly above 300 °C, which is always higher than that from RV, mainly attributed to the thermal decomposition of tar.⁴³ Therefore, the NH₃ production may be another reason for the decrease of HCN from ADV above 600 °C because both the gaseous groups derive from the decomposition of the tar. The accumulative absorbance of NH₃ from food waste and vinasse increases by 24.5 and 276.2%, respectively, but slight change presents from cow manure after AD, showing that AD has a considerable effect on the NH₃ production from food waste and vinasse. N 1s spectra reveal that the peak intensity of amine-N in ADFW and ADV become stronger than that in RFW and RV (Figure S3), supplying additional evidence for higher NH₃ yield from ADFW and ADV. The discharge of NH₃ into the atmosphere caused a variety of pollution such as a reduction in photosynthetic rate and biodiversity, eutrophication of lakes or coastal waters, and soil acidification.⁴⁴ Therefore, special attention needs to be paid to NH₃ emissions during the energy utilization of digestate-based syngas.

As shown in Figure 3, the accumulative absorbance of HNCO in RFW, RV, and RCM decreases by 20.9, 40.4, and 15.3%, respectively, after AD. HNCO is derived from nitrile-N during pyrolysis.⁴⁵ Therefore, the results implied that AD causes a decrease in the nitrile-like groups of the organic wastes. NO is one of the least-nitrogen-containing gases, accounting for 1.8–5.4% of all of the gases. The NO generation occurs mainly between 300 and 600 °C, possibly a result of the reaction between the N-containing compound and the •OH generated when the C–OH bond is broken.⁴⁶

3.3.3. Gaseous S-Containing Groups. Changes in the instantaneous and accumulative absorbance of S-containing gaseous products of the six substrates with different temper-

atures are shown in Figure 4 and Table 3. The accumulative absorbance of S-containing gaseous products from ADFW and ADV decreases by 5.6 and 22.0%, respectively, and that from ADCM increases by 9.1%, compared with raw substrates. As shown in Table 1, the ADCM has the highest sulfur content in all of the substrates and digestates. As shown in the S 2p XPS spectra in Figure S4, the peak intensity of S-containing groups of cow manure becomes stronger after AD, corresponding to an increase in S-containing gaseous products of cow manure after AD. Liu et al.³⁴ reported that S-containing gases such as H₂S, SO₂, and COS are mainly produced from the decomposition of sulfates and sulfur-containing organic compounds. Therefore, the reduction of S-containing gaseous products from food wastes and vinasse after AD may be attributed to the transformation of sulfates and sulfur-containing organic compounds to H₂S discharged with the biogas during anaerobic digestion.

The SO₂ accounts for large proportion of the total S-containing gas, and its percentage reaches 61.9–67.6%. As shown in Figure 4 and Table 3, AD causes a decrease in the accumulative absorbance of SO₂ from food waste and vinasse by 4.4 and 28.5%, respectively, while an increase from cow manure by 9.3%. The accumulative absorbance of H₂S from RFW and RV decreases by 9.7 and 30.8%, respectively, while that from RCM increases by 11.5% after AD. The results show that compared with RV and RCM, RFW has less change in the generation of SO₂ and H₂S after AD. The studies have reported that RV contains lots of K, Ca, and Mg,^{30,47} and compared with RV, the intensity of Ca is higher in ADV (Figure S2). Ca and Mg can react with S-containing acid gas, and thus sulfur remains in the solid residue in the form of metal sulfides, leading to the reduction of SO₂ and H₂S released from ADV.^{15,30} In addition, Cheah et al.⁴⁸ have reported that in the pyrolysis process of some herbaceous materials (such as corn stover), high levels of silicon in corn stover can compete with cations such as Ca, K, Mg, and Na, resulting in more sulfur entering the syngas. The corn stover is a kind of cattle feed, leading to the deposition of silicon in RCM. As a result, the SO₂ and H₂S released from RCM increase after AD.

The accumulative absorbance of COS from RFW decreases by 3.7% but increases from RV and RCM by 18.5 and 4.1% after AD, respectively. Compared with that from the food waste and cow manure, the COS from the vinasse has a more obvious increase after AD, which happens in the temperature range of 200–600 °C. COS is mainly produced through the following two reactions (e.g., eqs 3 and 4)⁴⁹



3.4. Implication of the Study. Due to the different contents of carbohydrate, protein, cellulose, and lipid, the effects of AD on the sequential pyrolysis from food waste, vinasse, and cow manure are different. Syngas is an important volatile product with a calorific value of 10–14 MJ/kg, which is a good fuel for power generation and cooking. The combustion performance of syngas is mainly related to C-containing gas, the high heating values of CH₄ is 12.68 MJ/Nm³.⁵⁰ In the C-containing gas, AD reduces the CH₄ content from the sequential pyrolysis of food waste, vinasse, and cow manure, causing the low combustion performance of syngas from digestates. After AD, the total concentration of N-containing

gases in vinasse increases significantly with the value of 40.1%, so it is worth noting that N-containing gas from pyrolysis of vinasse digestates may cause lake eutrophication and soil acidification, especially for NH_3 and HCN. They are easily soluble in water and thus may be removed by adding a water scrubber in the pyrolysis process of ADV.^{22,51} In addition, AD causes an increase in the total quantity of S-containing components in the syngas of cow manure. Liu et al.⁵² found that the addition of CaO during the pyrolysis process promotes the formation of thermally stable sulfides and sulfates and thus significantly reduces the generation of S-containing gases. Therefore, the release of S-containing gas can be reduced through the CaO addition during the pyrolysis process of ADCM.

4. CONCLUSIONS

AD has differential effects on the C-, N-, and S-containing gaseous products in the pyrolysis of food waste, vinasse, and cow manure due to their diverse chemical compositions. The difference in the weight loss of the three organic substances mainly exists in the second stage, and the weight-loss rate of raw and anaerobically digested food waste and vinasse is higher than that of RCM and ADCM. In the C-containing gas, AD reduce the CH_4 content from RFW, RV and RCM, implying a low combustion performance of digestate-based syngas. After AD, the total content of the N-containing gases from vinasse increased significantly by 40.1%. The total amount of S-containing components in the syngas from ADCM increased by 9.1%. The findings supply new insight into the effect of AD on the sequential pyrolysis of organic solid wastes in the term of syngas and provide an important foundation for designing the optimized pyrolysis process of the digestates.

■ ASSOCIATED CONTENT

SI Supporting Information

The Supporting Information is available free of charge at <https://pubs.acs.org/doi/10.1021/acsomega.1c02678>.

Tentative identification of pyrolysis gaseous products based on FTIR peak wavenumber; binding energy, relative content, and chemical states of C, O, N, and S in the raw materials and digestates; changes in C-containing gaseous products (CH_3OH , CH_3CHO , CH_3COOH) during pyrolysis; XPS, N 1s XPS spectra, and S 2p XPS spectra of RFW, ADFW, RV, ADV, RCM, and ADCM (PDF)

■ AUTHOR INFORMATION

Corresponding Author

Xiaowei Li – School of Environmental and Chemical Engineering, Key Laboratory of Organic Compound Pollution Control, Ministry of Education, Shanghai University, Shanghai 200444, China; orcid.org/0000-0002-5778-0947; Phone: 86-021-66137746; Email: lixiaowei419@shu.edu.cn

Authors

Lianpei Zou – School of Environmental and Chemical Engineering, Key Laboratory of Organic Compound Pollution Control, Ministry of Education, Shanghai University, Shanghai 200444, China

Lin Song – School of Environmental and Chemical Engineering, Key Laboratory of Organic Compound Pollution

Control, Ministry of Education, Shanghai University, Shanghai 200444, China

Man Li – School of Environmental and Chemical Engineering, Key Laboratory of Organic Compound Pollution Control, Ministry of Education, Shanghai University, Shanghai 200444, China

Xuan Wang – School of Environmental and Chemical Engineering, Key Laboratory of Organic Compound Pollution Control, Ministry of Education, Shanghai University, Shanghai 200444, China

Xiang Huang – School of Environmental and Chemical Engineering, Key Laboratory of Organic Compound Pollution Control, Ministry of Education, Shanghai University, Shanghai 200444, China

Yaning Zhang – School of Environmental and Chemical Engineering, Key Laboratory of Organic Compound Pollution Control, Ministry of Education, Shanghai University, Shanghai 200444, China

Bin Dong – College of Environmental Science and Engineering, Tongji University, Shanghai 200092, China

John Zhou – School of Civil and Environmental Engineering, University of Technology Sydney, Sydney, NSW 2007, Australia

Complete contact information is available at: <https://pubs.acs.org/10.1021/acsomega.1c02678>

Notes

The authors declare no competing financial interest.

■ ACKNOWLEDGMENTS

The work was financially supported by the Shanghai Committee of Science and Technology (19DZ1204702), the National Natural Scientific Foundation of China (5207126), the National Key Research and Development Program of China (2018YFC1903201), and the Program of Shanghai Technology Research Leader Grant (17XD1420500).

■ REFERENCES

- (1) Girotto, F.; Alibardi, L.; Cossu, R. Food waste generation and industrial uses: A review. *Waste Manage.* **2015**, *45*, 32–41.
- (2) Sydney, E. B.; Larroche, C.; Novak, A. C.; Nouaille, R.; Sarma, S. J.; Brar, S. K.; Letti, L. A. J.; Soccol, V. T.; Soccol, C. R. Economic process to produce biohydrogen and volatile fatty acids by a mixed culture using vinasse from sugarcane ethanol industry as nutrient source. *Bioresour. Technol.* **2014**, *159*, 380–386.
- (3) Zhang, P.; Zhang, X.; Li, Y.; Han, L. Influence of pyrolysis temperature on chemical speciation, leaching ability, and environmental risk of heavy metals in biochar derived from cow manure. *Bioresour. Technol.* **2020**, *302*, No. 122850.
- (4) Ren, Y.; Yu, M.; Wu, C.; Wang, Q.; Gao, M.; Huang, Q.; Liu, Y. A comprehensive review on food waste anaerobic digestion: Research updates and tendencies. *Bioresour. Technol.* **2018**, *247*, 1069–1076.
- (5) Opatokun, S. A.; Strezov, V.; Kan, T. Product based evaluation of pyrolysis of food waste and its digestate. *Energy* **2015**, *92*, 349–354.
- (6) Tampio, E.; Salo, T.; Rintala, J. Agronomic characteristics of five different urban waste digestates. *J. Environ. Manage.* **2016**, *169*, 293–302.
- (7) Nansubuga, I.; Banadda, N.; Ronsse, F.; Verstraete, W.; Rabaey, K. Digestion of high rate activated sludge coupled to biochar formation for soil improvement in the tropics. *Water Res.* **2015**, *81*, 216–222.
- (8) Teglia, C.; Tremier, A.; Martel, J.-L. Characterization of Solid Digestates: Part 1, Review of Existing Indicators to Assess Solid Digestates Agricultural Use. *Waste Biomass Valorization* **2011**, *2*, 43–58.

- (9) Lu, J.-S.; Chang, Y.; Poon, C.-S.; Lee, D.-J. Slow pyrolysis of municipal solid waste (MSW): A review. *Bioresour. Technol.* **2020**, *312*, No. 123615.
- (10) Cao, Y.; Pawłowski, A. Sewage sludge-to-energy approaches based on anaerobic digestion and pyrolysis: Brief overview and energy efficiency assessment. *Renewable Sustainable Energy Rev.* **2012**, *16*, 1657–1665.
- (11) Kim, S.; Lee, Y.; Andrew Lin, K.-Y.; Hong, E.; Kwon, E. E.; Lee, J. The valorization of food waste via pyrolysis. *J. Cleaner Prod.* **2020**, *259*, No. 120816.
- (12) Inyang, M.; Gao, B.; Ding, W.; Pullammanappallil, P.; Zimmerman, A. R.; Cao, X. Enhanced Lead Sorption by Biochar Derived from Anaerobically Digested Sugarcane Bagasse. *Sep. Sci. Technol.* **2011**, *46*, 1950–1956.
- (13) Liang, J.; Lin, Y.; Wu, S.; Liu, C.; Lei, M.; Zeng, C. Enhancing the quality of bio-oil and selectivity of phenols compounds from pyrolysis of anaerobic digested rice straw. *Bioresour. Technol.* **2015**, *181*, 220–223.
- (14) Tayibi, S.; Monlau, F.; Marias, F.; Cazaudehore, G.; Fayoud, N. E.; Oukarroum, A.; Zeroual, Y.; Barakat, A. Coupling anaerobic digestion and pyrolysis processes for maximizing energy recovery and soil preservation according to the circular economy concept. *J. Environ. Manage.* **2021**, *279*, No. 111632.
- (15) Meng, X. Biomass Gasification: The Understanding of Sulfur, Tar, and Char Reaction in Fluidized Bed Gasifiers. Ph.D Thesis, Delft University of Technology; Netherlands, 2012.
- (16) Cantrell, K. B.; Hunt, P. G.; Uchimiya, M.; Novak, J. M.; Ro, K. S. Impact of pyrolysis temperature and manure source on physicochemical characteristics of biochar. *Bioresour. Technol.* **2012**, *107*, 419–428.
- (17) Ateş, F.; Miskolczi, N.; Borsodi, N. Comparison of real waste (MSW and MPW) pyrolysis in batch reactor over different catalysts. Part I: Product yields, gas and pyrolysis oil properties. *Bioresour. Technol.* **2013**, *133*, 443–454.
- (18) Fernández, Y.; Menéndez, J. A. Influence of feed characteristics on the microwave-assisted pyrolysis used to produce syngas from biomass wastes. *J. Anal. Appl. Pyrolysis* **2011**, *91*, 316–322.
- (19) Zong, P.; Jiang, Y.; Tian, Y.; Li, J.; Yuan, M.; Ji, Y.; Chen, M.; Li, D.; Qiao, Y. Pyrolysis behavior and product distributions of biomass six group components: Starch, cellulose, hemicellulose, lignin, protein and oil. *Energy Convers. Manage.* **2020**, *216*, No. 112777.
- (20) Li, X.; Mei, Q.; Dai, X.; Ding, G. Effect of anaerobic digestion on sequential pyrolysis kinetics of organic solid wastes using thermogravimetric analysis and distributed activation energy model. *Bioresour. Technol.* **2017**, *227*, 297–307.
- (21) Luckos, A.; Shaik, M.; van Dyk, J. Gasification and Pyrolysis of Coal. In *Handbook of Combustion*, 1st ed.; Wiley-VCH: Weinheim, 2010; pp 325–364.
- (22) Chen, H.; Namioka, T.; Yoshikawa, K. Characteristics of tar, NO_x precursors and their absorption performance with different scrubbing solvents during the pyrolysis of sewage sludge. *Appl. Energy* **2011**, *88*, 5032–5041.
- (23) Liu, H.; Zhang, Q.; Xing, H.; Hu, H.; Li, A.; Yao, H. Product distribution and sulfur behavior in sewage sludge pyrolysis: Synergistic effect of Fenton peroxidation and CaO conditioning. *Fuel* **2015**, *159*, 68–75.
- (24) Cai, J.; Xu, D.; Dong, Z.; Yu, X.; Yang, Y.; Banks, S. W.; Bridgwater, A. V. Processing thermogravimetric analysis data for isoconversional kinetic analysis of lignocellulosic biomass pyrolysis: Case study of corn stalk. *Renewable Sustainable Energy Rev.* **2018**, *82*, 2705–2715.
- (25) Ong, H. C.; Chen, W.-H.; Singh, Y.; Gan, Y. Y.; Chen, C.-Y.; Show, P. L. A state-of-the-art review on thermochemical conversion of biomass for biofuel production: A TG-FTIR approach. *Energy Convers. Manage.* **2020**, *209*, No. 112634.
- (26) Li, X.; Chen, L.; Dai, X.; Mei, Q.; Ding, G. Thermogravimetry–Fourier transform infrared spectrometry–mass spectrometry technique to evaluate the effect of anaerobic digestion on gaseous products of sewage sludge sequential pyrolysis. *J. Anal. Appl. Pyrolysis* **2017**, *126*, 288–297.
- (27) Yao, Q.; Sun, M.; Gao, J.; Wang, R.; Zhang, Y.; Xu, L.; Ma, X. Organic sulfur compositions and distributions of tars from the pyrolysis of solvent pretreatment vitrinite of high sulfur coal. *J. Anal. Appl. Pyrolysis* **2019**, *139*, 291–300.
- (28) Patuzzi, F.; Roveda, D.; Mimmo, T.; Karl, J.; Baratieri, M. A comparison between on-line and off-line tar analysis methods applied to common reed pyrolysis. *Fuel* **2013**, *111*, 689–695.
- (29) Pramanik, S. K.; Suja, F. B.; Zain, S. M.; Pramanik, B. K. The anaerobic digestion process of biogas production from food waste: Prospects and constraints. *Bioresour. Technol. Rep.* **2019**, *8*, No. 100310.
- (30) Parsaee, M.; Kiani Deh Kiani, M.; Karimi, K. A review of biogas production from sugarcane vinasse. *Biomass Bioenergy* **2019**, *122*, 117–125.
- (31) Li, Y.; Achinas, S.; Zhao, J.; Geurkink, B.; Krooneman, J.; Willem Euvierink, G. J. Co-digestion of cow and sheep manure: Performance evaluation and relative microbial activity. *Renewable Energy* **2020**, *153*, 553–563.
- (32) Yang, C.; Li, R.; Zhang, B.; Qiu, Q.; Wang, B.; Yang, H.; Ding, Y.; Wang, C. Pyrolysis of microalgae: A critical review. *Fuel Process. Technol.* **2019**, *186*, 53–72.
- (33) Ronsse, F.; van Hecke, S.; Dickinson, D.; Prins, W. Production and characterization of slow pyrolysis biochar: influence of feedstock type and pyrolysis conditions. *GCB Bioenergy* **2013**, *5*, 104–115.
- (34) Tang, Y.; Li, X.; Dong, B.; Huang, J.; Wei, Y.; Dai, X.; Dai, L. Effect of aromatic repolymerization of humic acid-like fraction on digestate phytotoxicity reduction during high-solid anaerobic digestion for stabilization treatment of sewage sludge. *Water Res.* **2018**, *143*, 436–444.
- (35) Hu, M.; Chen, Z.; Guo, D.; Liu, C.; Xiao, B.; Hu, Z.; Liu, S. Thermogravimetric study on pyrolysis kinetics of *Chlorella pyrenoidosa* and bloom-forming cyanobacteria. *Bioresour. Technol.* **2015**, *177*, 41–50.
- (36) Cuetos, M. J.; Gomez, X.; Otero, M.; Moran, A. Anaerobic digestion of solid slaughterhouse waste: study of biological stabilization by Fourier Transform infrared spectroscopy and thermogravimetry combined with mass spectrometry. *Biodegradation* **2010**, *21*, 543–556.
- (37) Yuan, X.; He, T.; Cao, H.; Yuan, Q. Cattle manure pyrolysis process: Kinetic and thermodynamic analysis with isoconversional methods. *Renewable Energy* **2017**, *107*, 489–496.
- (38) Cheng, F.; Bayat, H.; Jena, U.; Brewer, C. E. Impact of feedstock composition on pyrolysis of low-cost, protein- and lignin-rich biomass: A review. *J. Anal. Appl. Pyrolysis* **2020**, *147*, No. 104780.
- (39) Zhou, S.; Han, L.; Huang, G.; Yang, Z.; Peng, J. Pyrolysis characteristics and gaseous product release properties of different livestock and poultry manures: Comparative study regarding influence of inherent alkali metals. *J. Anal. Appl. Pyrolysis* **2018**, *134*, 343–350.
- (40) Liu, Q.; Wang, S.; Zheng, Y.; Luo, Z.; Cen, K. Mechanism study of wood lignin pyrolysis by using TG–FTIR analysis. *J. Anal. Appl. Pyrolysis* **2008**, *82*, 170–177.
- (41) Li, X.; Li, Z.; Dai, X.; Dong, B.; Tang, Y. Micro-aerobic digestion of high-solid anaerobically digested sludge: Further stabilization, microbial dynamics and phytotoxicity reduction. *RSC Adv.* **2016**, *6*, 76748–76758.
- (42) Wang, X.; Sheng, L.; Yang, X. Pyrolysis characteristics and pathways of protein, lipid and carbohydrate isolated from microalgae *Nannochloropsis* sp. *Bioresour. Technol.* **2017**, *229*, 119–125.
- (43) Zhang, J.; Tian, Y.; Zhu, J.; Zuo, W.; Yin, L. Characterization of nitrogen transformation during microwave-induced pyrolysis of sewage sludge. *J. Anal. Appl. Pyrolysis* **2014**, *105*, 335–341.
- (44) Chen, S.; Cheng, M.; Guo, Z.; Xu, W.; Du, X.; Li, Y. Enhanced atmospheric ammonia (NH₃) pollution in China from 2008 to 2016: Evidence from a combination of observations and emissions. *Environ. Pollut.* **2020**, *263*, No. 114421.
- (45) Tian, Y.; Zhang, J.; Zuo, W.; Chen, L.; Cui, Y.; Tan, T. J. Nitrogen Conversion in Relation to NH₃ and HCN during

Microwave Pyrolysis of Sewage Sludge. *Environ. Sci. Technol.* **2013**, *47*, 3498–3505.

(46) Tian, K.; Liu, W. J.; Qian, T. T.; Jiang, H.; Yu, H. Q. Investigation on the evolution of N-containing organic compounds during pyrolysis of sewage sludge. *Environ. Sci. Technol.* **2014**, *48*, 10888–10896.

(47) Zhang, H.; Itakura, A.; Matsuto, T. Carbon and nutrient distributions between gas, solid, and liquid in anaerobic digestion facilities for various types of organic waste. *Biosyst. Eng.* **2012**, *113*, 11–21.

(48) Cheah, S.; Malone, S. C.; Feik, C. J. Speciation of sulfur in biochar produced from pyrolysis and gasification of oak and corn stover. *Environ. Sci. Technol.* **2014**, *48*, 8474–8480.

(49) Duan, L.; Zhao, C.; Wu, Z.; Qu, C.; Chen, X. Investigation on coal pyrolysis in CO₂ atmosphere. *Energy Fuels* **2009**, *23*, 3826–3830.

(50) Font-Palma, C. Methods for the Treatment of Cattle Manure—A Review. *C* **2019**, *5*, 27.

(51) Phuphuakrat, T.; Namioka, T.; Yoshikawa, K. Tar removal from biomass pyrolysis gas in two-step function of decomposition and adsorption. *Appl. Energy* **2010**, *87*, 2203–2211.

(52) Liu, H.; Zhang, Q.; Hu, H.; Xiao, R.; Li, A.; Qiao, Y.; Yao, H.; Naruse, I. Dual role of conditioner CaO in product distributions and sulfur transformation during sewage sludge pyrolysis. *Fuel* **2014**, *134*, 514–520.